Both DNA Polymerases δ and ε Contact Active and Stalled Replication Forks differently

Chuanhe Yu[1,2], Haiyun Gan[2,3], Zhiguo Zhang[3]

[1]Department of Biochemistry and Molecular Biology, Mayo Clinic, Rochester, MN, 55905, USA

[3]Institute for Cancer Genetics, Department of Pediatrics, Department of Genetics and Development, Columbia University, 1130 St. Nicholas Avenue, Irving Cancer Research Center ICRC 407A, New York, NY10032

[2]Equal contribution

[*]Corresponding author: zz2401@cumc.columbia.edu

(p): 212-851-4239

Running title: DNA polymerases configuration on replication fork

Key words: DNA replication, replication stress, DNA polymerase, ChIP-ssSeq, strand specific sequencing

Abstract

Three DNA polymerases (Pol α, Pol δ, and Pol ε) are responsible for eukaryotic genome duplication. When DNA replication stress is encountered, DNA synthesis stalls until the stress is ameliorated. However, it is not known whether there is a difference in the association of each polymerase with active and stalled replication forks. Here, we show that each DNA polymerase has distinct patterns of association with active and stalled replication forks. Pol α is enriched at extending Okazaki fragments of active and stalled forks. In contrast, although Pol δ contacts the nascent lagging strands of active and stalled forks, it binds to only the matured (and not elongating) Okazaki fragments of stalled forks. Pol ε has a greater contact with the nascent ssDNA of leading strand on active forks compared with stalled forks. We propose that the configuration of DNA polymerases at stalled forks facilitate resumption of DNA synthesis after stress removal.

Introduction

During eukaryotic genome duplication, replication stress is known to cause DNA synthesis to stall until the stress is alleviated. Replication stress includes lesions induced by endogenous and exogenous DNA-damaging agents, ribonucleotide mis-incorporation, and formation of secondary structures or DNA-RNA hybrids (1, 2). To better understand how genome integrity is maintained throughout replication stress, it is critical to determine how replisomes associate with DNA in active and stalled replication forks.

In budding yeast, DNA replication initiates at multiple sites, termed autonomously replicating sequences (ARSs) or replication origins. These origins are regulated temporally, with some origins firing early and others firing late in S phase of the cell cycle (3). In budding yeast, one of the primary responses to DNA replication stress is activation of the Mec1 and Rad53 kinase signaling cascade, a process equivalent to ataxia telangiectasia mutated− and Rad3-related (ATR) activation in human cells. Activated checkpoint kinases inhibit firing of late replication origins, maintain the stability of stalled replication forks, and help restart DNA synthesis.

DNA polymerases α, ε, and δ (Pol α, Pol ε, and Pol δ) are the main replicative DNA polymerases for eukaryotic nuclear genome, but other proteins are also involved in the process of DNA replication, including the Origin Recognition Complex (ORC) and replicative helicase minichromosome maintenance (MCM) proteins. In G1/S transition, MCM is activated through formation of the CMG complex (Cdc45, Mcm2-7, and GINS complex) and phosphorylation two kinases, CDK and DDK(4). Activated CMG helicase unwinds double-stranded DNA (dsDNA) at origins and recruits the single-stranded DNA (ssDNA)−binding protein RPA; RPA facilitates recruitment of Pol α, which synthesizes RNA primers followed by short DNA chain to initiate

63 leading strands and Okazaki fragment synthesis. Pol ε and Pol δ extend Pol α's products. In
64 budding yeast, based on mutation bias introduced by Pol ε and δ mutants, it was proposed that
65 Pol ε and δ are responsible for the synthesis of the leading and lagging strands, respectively (5-7).
66 Recently, by mapping ribonucleotides introduced by DNA Polε and Polδ mutants genome wide
67 in both budding yeast and fission yeast (8-11), it is deduced by that Polε and Polδ are involved in
68 synthesis of leading and lagging strand, respectively. We have shown that Pol ε and Pol δ are
69 enriched at nascent leading and lagging strands, respectively (12). However, a recent study of
70 budding yeast suggest that Pol δ is involved in the synthesis of both leading and lagging strands
71 and Pol ε is involved in DNA repair (13).

72

73 We and others have shown that proliferating cell nuclear antigen (PCNA), a processivity
74 factor for Pol ε and Pol δ, is unloaded from lagging strands of stalled DNA replication forks and
75 that this unloading is regulated by checkpoint kinases (12). Therefore, while replication proteins
76 still associate with replisomes under stress so that DNA synthesis can resume once DNA
77 replication stress is terminated, their contacts with DNA at stalled fork may differ from those
78 with active forks. To analyze the interaction of DNA polymerases with replication forks in
79 budding yeast, we evaluated the association of Pol α, Pol ε, and Pol δ with DNA in active and
80 hydroxyurea (HU)-stalled replication forks by using chromatin immunoprecipitation plus strand-
81 specific next-generation DNA sequencing (ChIP-ssSeq). Here, we report an in-depth analysis of
82 protein ChIP-ssSeq datasets, which reveals distinct pattern of interaction of Pol δ and Pol ε with
83 DNA at active and stalled replication forks. We suggest that these changes in contact with DNA

84 directly or indirectly help maintain stability of stalled forks and facilitate the resumption of DNA
85 synthesis after amelioration of replication stress.

86

87 **Methods**

88 **Yeast strains**

89 Yeast strains used in this study were derived from W303 (*leu2-3, 112 ura3-1 his3-11, trp1-1,*
90 *ade2-1 can1-100*). Genotypes are listed in Supplemental Table 1.

91

92 **ChIP-ssSeq Procedure**

93 ChIP-ssSeq experiments were performed as described previously (12). Briefly, α factor was used
94 to synchronize yeast cells at G1 (5 μg/mL and 50 ng/mL for wild-type *BAR* and *bar1* mutant
95 strains, respectively). To analyze the association of proteins with active forks, G1-arrested cells
96 were released into chilled (16°C) YPD medium containing 400 mg/L bromodeoxyuridine (BrdU),
97 and samples were collected at different time points. We treated cells with HU, an inhibitor of
98 ribonucleotide reductase, to deplete cells of dNTP. Thus, HU stalls the progression of DNA
99 replication forks and inhibits the firing of late replication origins (14, 15). To analyze protein
100 association with HU-stalled forks, cells were released into fresh medium containing 400 mg/L
101 BrdU and 0.2M HU for 45 minutes. To perform ChIP, samples were incubated with 1%
102 paraformaldehyde at 25°C for 20 minutes and then quenched with 0.125 M glycine for 5 minutes.
103 Cells were lysed with glass beads, and the chromatin pellet was washed and sonicated to shear

DNA to an average fragment size of about 200-400 bp. Sheared chromatin was immunoprecipitated with anti-FLAG antibody F1804 or anti-RPA antibody (gift of Dr Steven Brill). After extensive washing, cross-links of the immunoprecipitated chromatin were reversed. DNA was recovered with the Chelex-100 protocol (16). Recovered DNA was purified with a PCR purification kit (Qiagen). ChIP DNA was used to Q-PCR analysis (Supplemental Table 2) and were treated at 95°C for 5 min before used for library preparation of ssDNA in accordance with previously published procedures (17).

ChIP-ssSeq sequencing and analysis

The ssDNA libraries were sequenced using paired-end sequencing on Illumina Hi-Seq 2000 or 2500 machines. Reads were first mapped to the yeast genome (sacCer3) using Bowtie2 software (18). Consistent pair-end reads were chosen for subsequent analysis. We noted that after removal of duplicated reads, pair-end reads with the same ends were rarely detected in our samples even for Mcm6 ChIP-seq using G1 cells. This is likely due to the fact that chromatin was sheared by sonication and the ends were processed during library preparation. The genome-wide read coverage of Watson and Crick strands was calculated by BEDTools (19). The reads of the Watson and Crick strands were merged for peak calling by using MACS software (20).

We used our previously mapped DNA origins dataset for analysis (12). To calculate the average bias pattern, the average $\log_2$ ratios of sequencing reads of Watson strand over Crick strand surrounding 134 early replication origins (±10 Kb and ±30 Kb of HU-stalled and active forks,

125 respectively) were calculated using a sliding window of 200-bp. The duplicate reads were
126 excluded from calculation. These ratios were then normalized against the corresponding input to
127 obtain the average bias pattern of ChIP-ssSeq. To analyze bias at individual origins, each peak
128 region was separated into 4 quadrants: Watson strand at the left (WL) and right (WR) of an
129 origin and Crick strand at the left (CL) and right (CR) of an origin. The number of sequence
130 reads in each quadrant was counted. The binomial distribution was used to calculate the *P* value
131 to determine whether sequence reads at leading strand (WL+CR) were different from those of the
132 lagging strand (WR+CL) at each replication fork. The $\log_2$ ratio ($\log_2$ [(WL+CR)/(WR+CL)]) at
133 each replication origin was calculated and used to determine whether a ChIP-ssSeq peak had a
134 positive or negative strand bias.

135 Published dataset used in this study: Gene Expression Omnibus under accession number
136 GSE52614.

137

138 **Results**

139 **Rationale for analyzing replication proteins using ChIP-ssSeq**

140 ChIP-sequencing (ChIP-seq) has been widely used to study the association pattern of a protein of
141 interest with chromatin (21). Most ChIP-seq libraries are prepared using protocols that involve
142 ligation of dsDNA, which often leads to loss of ssDNA and strand-specific information (Fig. 1A).
143 During DNA replication, dsDNA is unwound to generate ssDNA, which serves as the template
144 for DNA synthesis. In the process, replication proteins, including ssDNA-binding proteins RPA
145 and DNA polymerases, may partially interact with the ssDNA or DNA-RNA hybrids. In addition,

DNA replication forks consist of leading and lagging strand DNA synthesis, and strand-specific information helps elucidate how a protein interacts with forks.

We previously reported development of the enrichment and sequencing protein−associated nascent DNA (eSPAN) method, which detects the association of a replication protein with nascent leading/lagging strand DNA (Fig.1B, right panel) (12). However, this method loses the information on how a protein interacts with ssDNA, which is prevalent at DNA replication forks. We also generated ChIP-ssSeq datasets during the process of obtaining eSPAN datasets. Briefly, protein ChIP DNA was denatured and ligated to the 3′ end of an adaptor (oligo) (Illumina) with an ssDNA ligase; ssDNA was then converted into dsDNA and ligated to a second adaptor (17, 22). The sequence reads were mapped to the Watson and Crick strands of the yeast genome (Fig. 1B). Since DNAs for a protein ChIP-ssSeq likely contain both template and nascent DNA (Fig.1B, left panel), ChIP-ssSeq will allow us to deduce how a DNA replication protein associates with single-stranded template DNA. As discussed and shown below, the ChIP-ssSeq and the eSPAN are two complementary methods, with each revealing unique information on the association of a protein at DNA replication forks.

RPA ChIP-ssSeq shows that RPA is enriched at the lagging strand template

We first analyzed Rfa1 ChIP-ssSeq datasets to gain insight into how RPA associates with DNA replication forks. Briefly, yeast cells were arrested at G1 and then released into early S phase in the presence of HU for 45 minutes. Rfa1 (the large subunit of the RPA complex) ChIP was

167 performed with G1 cells and early S-phase cells. Rfa1 was barely detectable at the replication
168 origin (*ARS607*) or at a distal site (ARS607+8 kb, unreplicated region) at G1 (Supplemental Fig.
169 1A and 1B). In contrast, Rfa1 was enriched 10-fold at *ARS607* compared with the distal site
170 (ARS607+8 kb) in the presence of HU (Supplemental Fig. 1B), indicating that RPA is recruited
171 to DNA replication forks during S phase. Under these conditions, replication checkpoint kinase
172 Rad53 is activated as shown by Western blot analysis of Rad53 (Supplemental Fig. 1C). In
173 addition, the fact that late origins were not fired under these conditions also reflects the
174 activation of Rad53 checkpoint kinase. Rfa1 ChIP-ssSeq peaks at *ARS510* and *ARS511* were
175 asymmetric surrounding each origin (Fig. 2A), consistent with RPA binding to ssDNA and not to
176 dsDNA. We note that a previous study shows that RPA binds asymmetrically to resected ssDNA
177 in a double-strand break site (23).

178

179 To analyze Rfa1 ChIP-ssSeq results quantitatively at a genome-wide scale, we first
180 calculated the average bias pattern, which is the average $\log_2$ ratio of sequencing reads of Watson
181 strand over Crick strand using 200-bp sliding window surrounding 134 early replication origins.
182 The average bias pattern of Rfa1 ChIP-ssSeq peaks indicated that on the right side of origin,
183 RPA bound more to the Watson strand, whereas on the left side of origin, it bound more to the
184 Crick strand (Fig. 2B). We categorized this finding as a positive (+) bias pattern to differentiate it
185 from the leading-strand bias pattern revealed by the eSPAN method, which detects the
186 association of a protein with newly synthesized DNA (12). As controls, the Rfa1 ChIP-ssSeq
187 using G1 cells did not show any bias (Fig. 2B), suggesting that bias seen in early S phase reflects
188 how RPA associates with DNA replication forks in the presence of HU. We also analyzed the

bias pattern of Rfa1 ChIP-ssSeq peaks at each of the 134 individual replication origins (Fig. 2C). Rfa1 ChIP-ssSeq peaks showed (+) bias for most origins (n=89 [66%]), whereas the Rfa1 ChIP-ssSeq using G1 phase cells showed no bias for the majority of origins (n=119 [89%]). These results support the idea that RPA binds ssDNA of DNA replication forks stalled by HU.

While RPA is known to bind single-stranded template DNA, it may also contact nascent DNA at replication forks indirectly through protein-protein interactions. Indeed, RPA eSPAN reveals that RPA bind more to nascent lagging strands (12). Rfa1 ChIP-DNA contains the template strand and the nascent strand DNA. Two potential mechanisms account for the (+) bias pattern of Rfa1 ChIP-ssSeq peaks. First, (+) bias may indicate that more RPA binds to the lagging strand template than to the corresponding leading strand template (Fig. 2D). Second, RPA may bind more nascent leading strands than the corresponding nascent lagging strands. However, the later explanation contradicts the RPA eSPAN results outlined above (12) (Fig 2D). Based on our Rfa1 ChIP-ssSeq and Rfa1 eSPAN results, we suggest that more RPA binds lagging strand template than leading strand template of HU-stalled forks (Fig. 2D). The above RPA ChIP experiment is under HU condition. We also performed the RPA ChIP-ssSeq under normal condition. The results showed the same (+) bias pattern (Supplemental Fig. 1D-E), suggesting that more RPA are enriched at lagging strand template compared to leading strand template at both active and HU stalled forks. This explanation is consistent with the proposed model of RPA preferentially binding the lagging template strand to protect gaps between Okazaki fragments (24). To our knowledge, the result is the first experimental demonstration that more RPA binds lagging strand template than leading strand template. In addition to DNA

211 replication, RPA is also involved in DNA repair process and activation of DNA replication
212 checkpoint (25, 26).

213

214 **PCNA ChIP-ssSeq shows no strand bias at replication forks**

215 We analyzed PCNA ChIP-ssSeq datasets obtained from cells cultured with or without HU. No
216 obvious strand bias was observed from the analysis of the average bias pattern of all early
217 replication origins or the analysis of the bias pattern of individual origins (Supplemental Fig. 2A-
218 C). These results indicate that PCNA, a processivity factor of DNA polymerases that is loaded
219 onto primer-template junctions, contacts dsDNA including both template and nascent DNA at
220 active and HU-stalled replication forks.

221

222 **MCM ChIP-ssSeq shows no strand bias at stalled replication forks**

223 Analysis of Mcm6 ChIP-ssSeq showed no significant strand bias of HU-stalled forks
224 (Supplemental Fig. 2D-F), suggesting that the MCM helicase binds to dsDNA. Similar results
225 were obtained for Mcm4 ChIP-ssSeq (Supplemental Fig. 2D-F). This observation seems to
226 contradict the idea that the MCM complex travels along the leading strand (12, 27), and our
227 eSPAN results showing that MCM associates preferentially with nascent leading strand DNA
228 compared with nascent lagging strand DNA. One likely explanation for our ChIP-ssSeq results is
229 that the MCM helicase, while encircling one leading template DNA strand, still makes indirect
230 contact with another lagging template strand of HU-stalled forks. Indeed, it has been shown that
231 MCM protein complex interacts with both Polε, which is enriched at leading strand, and Polα,

which is enriched at lagging strands (28-31). For the rest of our studies, we focused on analysis on how three DNA polymerases associate with active and HU-stalled replication forks.

Pol α ChIP-ssSeq indicates that Pol α preferentially binds to DNA-RNA hybrids at lagging strands of active and HU-stalled replication forks

Pol α was enriched at the early replication origin (*ARS607*) compared with the distal site (ARS607+8 kb) when cells were released from G1 to early S phase in the presence of HU (Supplemental Fig. 3A-B), consistent with the results that Polα associates with replicating DNA even in the presence of HU (32, 33). Inspection of Pol α ChIP-ssSeq at replication origins ARS510 and ARS511 showed that Pol α ChIP-ssSeq peaks showed a strong (+) bias pattern (Fig.3A and 3B). Analysis of the average bias pattern of 134 early replication origins confirmed that the (+) bias pattern of Pol α ChIP-ssSeq peaks at individual forks on a genome-wide scale (Fig. 3B), with 126 of 134 peaks (94%) showing (+) bias (Fig. 3C). We also determined how Pol α bound to active replication forks by performing ChIP-ssSeq using cells released into S phase without HU at a lower temperature (Fig. 3C and Supplemental Fig. 3C). The Pol α ChIP-ssSeq peaks also showed (+) bias based on the analysis of average bias pattern of early replication origins, as well as in the analysis of individual origins (Fig. 3C-E).

Pol α ChIPed DNA consists of the lagging strand template and newly synthesized RNA-DNA primer. The (+) bias pattern of Pol α ChIP-ssSeq peaks indicates that more Pol α binds to lagging strand template than to leading strand template of active and HU-stalled replication forks. Supporting this idea, the published Pol α eSPAN peaks indicate that Pol α physically binds more

to nascent lagging strands than to leading strands at active and HU-stalled replication forks (12) (Fig. 3B, E-F). Because Pol α is involved in the synthesis of RNA and DNA primers, the (+) bias indicates that Pol α binds to initiating Okazaki fragments at HU-stalled forks and to the elongating Okazaki fragments of active replication forks (Fig. 3F).

Pol δ is enriched at elongating Okazaki fragments of lagging strand template only of active replication forks

We next analyzed Pol δ (catalytic subunit) ChIP-ssSeq obtained using cells released from G1 arrest into early S phase in the presence of HU. Pol δ ChIP-PCR analysis showed that Pol δ was enriched at replication forks originating from *ARS607* comparing to the unreplicated distal site (ARS607+8 kb) (Supplemental Fig. 4A-B). Pol δ ChIP-ssSeq peaks at HU-stalled forks did not reveal any bias pattern based on analysis of the average bias of 134 forks from early replication origins or with analysis of individual origins (Fig. 4A-C), suggesting that Pol δ binds equally to Watson and Crick strands of HU-stalled replication forks. In contrast, Pol δ ChIP-ssSeq peaks at active replication forks without HU showed small, but consistent (+) bias in the analysis of the average bias pattern and of individual forks at all three-time points (Fig. 4B-C). The difference in Pol δ ChIP-ssSeq peak bias between active and HU-stalled forks was unlikely due to difference in input samples (Supplemental Fig. 4C). Thus, Pol δ differentially associates with DNA at active and HU-stalled replication forks

In principle, Pol δ binds both template and nascent DNA. Therefore, Pol δ ChIP-ssSeq peaks should show no bias at both active and HU-stalled forks. The eSPAN analysis of Pol δ indicates that Pol δ binds preferentially nascent lagging strand of HU-stalled and active replication forks (12) (Fig. 4B). We therefore deduce from the (+) bias pattern of Pol δ ChIP-ssSeq peaks that Pol δ associates with more lagging strand template of active forks, which most likely reflect that Pol δ can associates with newly initiated Okazaki fragments with only very short nascent RNA of active forks (Fig. 4D-E). In contrast, this mode of association of Pol δ is lost at HU-stalled forks, which provides an explanation for a lacking of bias of Pol δ ChIP-ssSeq peaks of HU-stalled forks. We have shown recently that the DNA polymerase clamp, PCNA, is unloaded from lagging strands of HU-stalled forks (12). PCNA is important for the activity of Pol δ, likely important for tethering Pol δ at DNA replication forks. Therefore, the unloading of PCNA from lagging strand of HU stalled forks may contribute to the loss of the association of Pol δ newly initiated Okazaki fragment at HU-stalled forks, whereas Pol α still binds.

Pol ε−DNA interaction is different for active and the HU-stalled replication forks.

After determining the association of Pol α and Pol δ with DNA, we next used ChIP-ssSeq to examine how Pol ε interacts with DNA. Pol ε ChIP-PCR analysis indicated that Pol ε bind to replicating DNA at HU-stalled replication forks (Supplemental Fig. 4A-B). Like Pol δ, Polε ChIP-ssSeq showed that Pol ε did not show significant bias at HU-stalled replication forks from early replication origins (Fig. 5A-C), indicating that Pol ε is cross-linked to dsDNA, including the template strand and nascent leading strand of HU-stalled replication forks. Remarkably, Pol ε

ChIP-ssSeq showed (+) bias at actively replicating forks at all time points considered (72, 84, and 96 minutes after release from G1) (Fig. 5B). The bias pattern was detected at the majority of individual origins (Fig. 5C), suggesting that the Pol ε-DNA interaction at active forks differs from that at stalled forks.

The above Pol ε ChIP-ssSeq analysis of HU-stalled and active replication forks were obtained from independent experiments and Pol ε ChIP-ssSeq bias is small. Therefore, we performed additional experiments to confirm that different association patterns of Pol ε with DNA changes in stalled vs active forks. Briefly, yeast cells were arrested in G1 with α factor and then released into HU-containing medium for 45 minutes. A fraction of cells were collected for Pol ε ChIP-ssSeq, and the remaining cells were released into fresh medium without HU. Samples were used to perform Pol ε ChIP-ssSeq at 3 time points after release from HU (20, 30, and 40 minutes) (Fig. 5D). Analysis of Pol ε ChIP-ssSeq datasets showed no bias pattern for peaks obtained using cells treated with HU, whereas peaks from cells after HU removal showed (+) bias (Fig 5E-G). We noticed that Polε ChIP-ssSeq at HU conditions shown in Fig. 5B and 5F appears to show opposite trend. This is likely due to the fact that Polε ChIP-ssSeq peaks at most origins showed indeterminable bias (no bias) and variations at a small number of origins contributes to the apparent changes in the insignificant bias pattern (compare Fig. 5C and Fig. 5G). Nonetheless, we observed very consistent results of Polε ChIP-ssSeq at active forks from each of the 3 time points of two independent experiments , supporting the idea that the association of Pol ε with DNA is altered when active forks become stall by HU treatment.

315 Once again, two potential models explain the (+) bias pattern of Pol ε ChIP-ssSeq peaks
316 (Fig. 5H). Based on Polε eSPAN results (12) (Fig. 5B), Polε binds preferentially to leading
317 strand. Therefore, it is possible that in addition to contact with leading strand DNA, Pol ε may
318 also directly contact the lagging strand template during normal replication. This mechanism is
319 unlikely because it is hard to put the Cdc45-MCM-GINS complex, which is known to associate
320 with Pol ε on the leading strand (29), in front of Pol ε. Second, Pol ε may not contact the leading
321 strand template tightly, binding only to nascent DNA on the leading strand of active forks (Fig.
322 5H). We suggest that this mode of interaction with leading nascent DNA facilitates its ability to
323 proofread or repair mis-incorporated nucleotides by using its 3′-to-5′ exonuclease activity (34).
324 At stalled fork, Pol ε may backtrack and associate with dsDNA including both template and
325 nascent strands (Fig. 5I).

326

327 **Discussion**

328 Our present study reveals several novel insights into the contacts of proteins with active and HU-
329 stalled forks. First, we provide the experimental evidence that RPA are enriched at lagging strand
330 template compared to the corresponding leading strand template, consistent with the replication
331 model on the role of RPA in DNA replication. Second, we show that Polα associates with
332 lagging strand template of both active and HU-stalled forks. Third, we show that both Polδ and
333 Pol ε bind to HU-stalled forks differently from active forks. Specifically, Polδ binds to both
334 initiating and elongating Okazaki fragments at active forks, and is likely lost/removed from
335 initiating Okazaki fragments at HU-stalled forks where Polα remains to be present. Polε likely

backtracks and associtates dsDNA at HU-stalled forks. These results provide insight into how DNA synthesis can resume soon after removal of HU-induced replication stress.

Advantages and limitations of ChIP-ssSeq method and its comparison with the eSPAN method

The library preparation of traditional ChIP-Seq includes steps for dsDNA repair and dsDNA ligation. During the sample preparation process, protein-bound ssDNA and strand-specific information is lost (Fig. 1A). Generally, this loss is not an issue because most proteins bind dsDNA. However, during DNA replication, dsDNA is transiently unwound into ssDNA. Therefore, determining whether a DNA replication protein binds to ssDNA will help elucidate its mode of action in DNA synthesis. Here, we used ChIP-ssSeq to gain insights into how DNA replication proteins bind to active and stalled replication forks. Since DNAs for protein ChIP-ssSeq potentially contain both template and nascent DNA, we analyzed ChIP-ssSeq peaks by calculating the average log2 ratio of sequence reads of Watson over Crick strand. If a protein contacts dsDNA including both template and nascent DNA, the ratio should be zero without any bias towards Watson or Crick strand. If a protein binds ssDNA, the average log2 ratio of sequence reads of Watson over Crick strand of ChIP-ssSeq peaks is not zero. Indeed, ssDNA-binding protein RPA ChIP-ssSeq peaks at both active and HU-stalled forks exhibit (+) bias, indicating that more RPA are present at lagging strand template than leading strand template, consistent with replication models of RPA in DNA replication.

We reported previously the development of the eSPAN method, which detects how a protein associates with newly synthesized DNA at DNA replication forks (12). Using this method, we detect the association of different DNA replication proteins with nascent leading or lagging strand of DNA replication forks. For instance, we observed that Polε and Polδ are enriched at nascent leading and lagging strand, respectively, consistent with their division of labor during DNA synthesis. Interestingly, we also show that RPA is enriched at lagging strand using eSPAN. This result appears to contradict the idea that RPA binds and stabilizes single-stranded template DNA. Using ChIP-ssSeq, we show that RPA is enriched at lagging strand template compared to leading strand template. One explanation for the apparent discrepancy for RPA ChIP-ssSeq and eSPAN results is that RPA binds preferentially to lagging strand template, but contacts nascent DNA indirectly, likely through other proteins. In this way, RPA eSPAN peaks show lagging strand bias. Similarly, the PCNA eSPAN results show that PCNA is enriched at nascent lagging strand DNA of active forks and nascent leading strand DNA at HU-stalled forks, suggesting that PCNA is unloaded from lagging strand of HU-stalled forks (12). However, PCNA ChIP-ssSeq peaks at HU-stalled forks show no bias pattern. One explanation is that PCNA contacts both template DNA and nascent DNA at HU-stalled forks, which gives rise to the no bias pattern of PCNA ChIP-ssSeq peaks. Therefore, the bias pattern of eSPAN peaks and ChIP-ssSeq peaks has a different meaning: the eSPAN peak bias indicates how a protein associates with nascent leading and lagging strands of DNA replication forks, whereas ChIP-ssSeq peak bias reflects how a protein binds to ssDNA and dsDNA. Together, these results comparing ChIP-ssSeq and eSPAN of different proteins including RPA, PCNA and MCM, PCNA and DNA polymerases (below) indicate that the ChIP-ssSeq and eSPAN methods provide complementary information on how a protein associates with DNA replication forks.

In theory, ChIP-ssSeq is suitable for studying DNA repair and RNA transcription when strand-specific information is needed. In fact, some reports indicated that similar ChIP-ssSeq approaches can study the DNA repair process (23, 35). These studies used either sticky end dsDNA adaptor ligation or intramolecular microhomology to generate libraries. We adopted the ssDNA library preparation method developed by Meyer et al (17), which was used to analyze highly damaged DNA from ancient human samples. The advantage of this method, compared with the 2 published ssDNA library preparation methods, is high efficiency. Meyer's method can generate libraries from very low quantities of DNA (22), and it therefore is very suitable for constructing libraries from the low amount of DNA isolated by ChIP experiments. We expect that ChIP-ssSeq may also yield useful information for other processes besides DNA replication and repair. For instance, allele-specific DNA methylation is known to occur frequently in mammalian cells (36). A combination of library preparation methods with immunoprecipitation of methylated DNA will, in principle, be able to differentiate between methylated and unmethylated alleles. Future studies are needed to test this idea.

Association of Pol α with active and HU-stalled replication forks

The Pol α-primase complex synthesizes primers for subsequent DNA synthesis by Pol δ and Pol ε, likely at the lagging and leading strands of DNA replication forks, respectively. Previously, we used the eSPAN method to show that Pol α-primase is enriched at the nascent lagging strand of the DNA replication fork; this finding was consistent with the classical replication models that

require a Pol α-primase complex for each Okazaki fragment (37, 38). In this study, we used the Pol α ChIP-ssSeq method to show that Pol α also binds more to the lagging strand template during DNA replication, further supporting the role of Pol α−primase in the classical DNA replication model. Interestingly, we observed that Pol α−primase remains binding to the lagging strand template at HU-stalled replication forks. We suggest that the association of Pol α-primase complex with the template strand under this condition may facilitate resumption of the replication process soon after amelioration of DNA replication stress. In addition, this association may serve as the target of cell cycle checkpoint kinases that regulate arrest of DNA replication forks during stress. Consistent with this idea, previous work has shown that primase connects DNA replication to the DNA damage response (39).

Altered association of Pol δ and Pol ε with DNA replication forks stalled by replication stress

Pol δ replicates both leading and lagging strands in the SV40 *in vitro* replication system (40-42). However, genetic evidence from the past decade supports Pol ε as the leading-strand replication enzyme in yeast (5, 6, 8, 43, 44) and Pol δ is responsible for replicating lagging-strand DNA. Recently, the division of labor between Pol ε and Pol δ in DNA synthesis has come into question with genetic analyses of mismatch repair−deficient DNA polymerase mutants (13). Therefore, several eukaryotic DNA replication models have been proposed (45). In every model, Pol ε is always physically linked with MCM helicase on the leading strand, regardless of whether it is the major active leading-strand DNA polymerase or just a repair enzyme. The result is fully compatible with our eSPAN data, indicating that Pol ε is enriched at the replicating leading

423 strands. In contrast, Pol δ is enriched at the nascent lagging strands of DNA replication forks.
424 We show here that Pol δ and Pol ε asymmetrically bind to DNA of active replication forks,
425 suggesting that these two polymerases also bind to ssDNA, but not solely to dsDNA at active
426 replication forks. In contrast, at HU-stalled forks, Pol δ and Pol ε predominantly were bound to
427 dsDNA. We suggest that at HU-stalled forks, Pol ε may backtrack to contact dsDNA.

428

429 Previous study has shown that MCM localization can be displaced several hundred base pairs
430 from the origin by transcription regulation (46). While it is possible that transcriptional alteration
431 during HU block contributes to the lack of bias Pol ε and Pol δ ChIP-ssSeq peaks at HU-stalled
432 forks, it is unlikely for the following reasons, First, we show that the Pol ε ChIP-ssSeq peak bias
433 pattern reappears after we release cells from HU block to fresh media, suggesting that Pol ε bias
434 is associated with active replication forks. Second, it is known that HU has no apparent effect on
435 initiation of DNA replication at early replication origins based on studies from many laboratories.
436 Moreover, the observation that transcription can shift MCM localization was made in *rat1*
437 mutant cells in which transcription termination was reduced, whereas at HU-stalled forks, we did
438 not observe such dramatic alterations in MCM distribution (12).

439

440 We noticed the bias of Polδ and Polε ChIP-ssSeq peaks at active forks is small compared to that
441 of Rfa1 or Polα. The small bias is not likely an artifact of calculation because we analyzed ChIP-
442 ssSeq data sets using two different methods. First, we used 200 bp sliding window to calculate
443 bias from either 10 or 30Kb surrounding each replication origins of HU-stalled and active forks,

444 respectively. The trend of each data point of Polδ and Polε ChIP-ssSeq show that the bias, while
445 small, is not random. Second, we also analyzed whether there exist bias of Polδ and Polε ChIP-
446 ssSeq peaks at individual replication forks (Fig. 4C, Fig. 5C and Fig. 5G) and found that the bias,
447 while small, is statistically significant. Unlike RPA that binds ssDNA and Polα that synthesizes
448 primers for Polδ and Polε, most Polδ and Polε likely still contact dsDNA including template
449 DNA and newly synthesized DNA. Therefore, it is not surprising that Polδ and Polε ChIP-ssSeq
450 bias is smaller than RPA or Polα. In conclusion, the bias changes at HU-stalled forks and active
451 forks of Polδ and Polε ChIP-ssSeq, while small, reflect the polymerase-DNA spatial contacts at
452 active forks.

453

454 **Acknowledgement**

455 We thank Dr. Oscar Aparicio for yeast strains and plasmids. We thank Dr. Steven Brill for the
456 anti-RPA antibody and Dr. June Oshiro for editing our manuscript.

457

458
459 **Competing financial interests**

460 The authors declare no competing financial interests

461

462

References

1. **Zeman MK, Cimprich KA.** 2014. Causes and consequences of replication stress. Nat Cell Biol **16:**2-9.
2. **Mazouzi A, Velimezi G, Loizou JI.** 2014. DNA replication stress: causes, resolution and disease. Exp Cell Res **329:**85-93.
3. **Aparicio OM.** 2013. Location, location, location: it's all in the timing for replication origins. Genes Dev **27:**117-128.
4. **Bell SD, Botchan MR.** 2013. The minichromosome maintenance replicative helicase. Cold Spring Harb Perspect Biol **5:**a012807.
5. **Pursell ZF, Isoz I, Lundstrom EB, Johansson E, Kunkel TA.** 2007. Yeast DNA polymerase epsilon participates in leading-strand DNA replication. Science **317:**127-130.
6. **Nick McElhinny SA, Gordenin DA, Stith CM, Burgers PM, Kunkel TA.** 2008. Division of labor at the eukaryotic replication fork. Mol Cell **30:**137-144.
7. **Stillman B.** 2008. DNA polymerases at the replication fork in eukaryotes. Mol Cell **30:**259-260.
8. **Clausen AR, Lujan SA, Burkholder AB, Orebaugh CD, Williams JS, Clausen MF, Malc EP, Mieczkowski PA, Fargo DC, Smith DJ, Kunkel TA.** 2015. Tracking replication enzymology in vivo by genome-wide mapping of ribonucleotide incorporation. Nat Struct Mol Biol **22:**185-191.
9. **Daigaku Y, Keszthelyi A, Muller CA, Miyabe I, Brooks T, Retkute R, Hubank M, Nieduszynski CA, Carr AM.** 2015. A global profile of replicative polymerase usage. Nat Struct Mol Biol **22:**192-198.
10. **Reijns MA, Kemp H, Ding J, de Proce SM, Jackson AP, Taylor MS.** 2015. Lagging-strand replication shapes the mutational landscape of the genome. Nature **518:**502-506.
11. **Koh KD, Balachander S, Hesselberth JR, Storici F.** 2015. Ribose-seq: global mapping of ribonucleotides embedded in genomic DNA. Nat Methods **12:**251-257, 253 p following 257.
12. **Yu C, Gan H, Han J, Zhou ZX, Jia S, Chabes A, Farrugia G, Ordog T, Zhang Z.** 2014. Strand-Specific Analysis Shows Protein Binding at Replication Forks and PCNA Unloading from Lagging Strands when Forks Stall. Mol Cell **56:**551-563.
13. **Johnson RE, Klassen R, Prakash L, Prakash S.** 2015. A Major Role of DNA Polymerase delta in Replication of Both the Leading and Lagging DNA Strands. Mol Cell **59:**163-175.
14. **Santocanale C, Diffley JF.** 1998. A Mec1- and Rad53-dependent checkpoint controls late-firing origins of DNA replication. Nature **395:**615-618.
15. **Shirahige K, Hori Y, Shiraishi K, Yamashita M, Takahashi K, Obuse C, Tsurimoto T, Yoshikawa H.** 1998. Regulation of DNA-replication origins during cell-cycle progression. Nature **395:**618-621.
16. **Nelson JD, Denisenko O, Bomsztyk K.** 2006. Protocol for the fast chromatin immunoprecipitation (ChIP) method. Nat Protoc **1:**179-185.
17. **Meyer M, Kircher M, Gansauge MT, Li H, Racimo F, Mallick S, Schraiber JG, Jay F, Prufer K, de Filippo C, Sudmant PH, Alkan C, Fu Q, Do R, Rohland N, Tandon A, Siebauer M, Green RE, Bryc K, Briggs AW, Stenzel U, Dabney J, Shendure J, Kitzman J, Hammer MF, Shunkov MV, Derevianko AP, Patterson N, Andres AM, Eichler EE, Slatkin M, Reich D, Kelso J, Paabo S.** 2012. A high-coverage genome sequence from an archaic Denisovan individual. Science **338:**222-226.
18. **Langmead B, Salzberg SL.** 2012. Fast gapped-read alignment with Bowtie 2. Nat Methods **9:**357-359.
19. **Quinlan AR, Hall IM.** 2010. BEDTools: a flexible suite of utilities for comparing genomic features. Bioinformatics **26:**841-842.
20. **Zhang Y, Liu T, Meyer CA, Eeckhoute J, Johnson DS, Bernstein BE, Nusbaum C, Myers RM, Brown M, Li W, Liu XS.** 2008. Model-based analysis of ChIP-Seq (MACS). Genome Biol **9:**R137.

21. **Barski A, Cuddapah S, Cui K, Roh TY, Schones DE, Wang Z, Wei G, Chepelev I, Zhao K.** 2007. High-resolution profiling of histone methylations in the human genome. Cell **129:**823-837.
22. **Gansauge MT, Meyer M.** 2013. Single-stranded DNA library preparation for the sequencing of ancient or damaged DNA. Nat Protoc **8:**737-748.
23. **Yamane A, Robbiani DF, Resch W, Bothmer A, Nakahashi H, Oliveira T, Rommel PC, Brown EJ, Nussenzweig A, Nussenzweig MC, Casellas R.** 2013. RPA accumulation during class switch recombination represents 5'-3' DNA-end resection during the S-G2/M phase of the cell cycle. Cell Rep **3:**138-147.
24. **O'Donnell M, Langston L, Stillman B.** 2013. Principles and concepts of DNA replication in bacteria, archaea, and eukarya. Cold Spring Harb Perspect Biol **5**.
25. **Marechal A, Zou L.** 2013. DNA damage sensing by the ATM and ATR kinases. Cold Spring Harb Perspect Biol **5**.
26. **Zou L, Elledge SJ.** 2003. Sensing DNA damage through ATRIP recognition of RPA-ssDNA complexes. Science **300:**1542-1548.
27. **Fu YV, Yardimci H, Long DT, Ho TV, Guainazzi A, Bermudez VP, Hurwitz J, van Oijen A, Scharer OD, Walter JC.** 2011. Selective bypass of a lagging strand roadblock by the eukaryotic replicative DNA helicase. Cell **146:**931-941.
28. **Langston LD, Zhang D, Yurieva O, Georgescu RE, Finkelstein J, Yao NY, Indiani C, O'Donnell ME.** 2014. CMG helicase and DNA polymerase epsilon form a functional 15-subunit holoenzyme for eukaryotic leading-strand DNA replication. Proc Natl Acad Sci U S A **111:**15390-15395.
29. **Sengupta S, van Deursen F, de Piccoli G, Labib K.** 2013. Dpb2 integrates the leading-strand DNA polymerase into the eukaryotic replisome. Curr Biol **23:**543-552.
30. **Gambus A, Jones RC, Sanchez-Diaz A, Kanemaki M, van Deursen F, Edmondson RD, Labib K.** 2006. GINS maintains association of Cdc45 with MCM in replisome progression complexes at eukaryotic DNA replication forks. Nat Cell Biol **8:**358-366.
31. **Gambus A, van Deursen F, Polychronopoulos D, Foltman M, Jones RC, Edmondson RD, Calzada A, Labib K.** 2009. A key role for Ctf4 in coupling the MCM2-7 helicase to DNA polymerase alpha within the eukaryotic replisome. EMBO J **28:**2992-3004.
32. **Cobb JA, Bjergbaek L, Shimada K, Frei C, Gasser SM.** 2003. DNA polymerase stabilization at stalled replication forks requires Mec1 and the RecQ helicase Sgs1. Embo Journal **22:**4325-4336.
33. **De Piccoli G, Katou Y, Itoh T, Nakato R, Shirahige K, Labib K.** 2012. Replisome stability at defective DNA replication forks is independent of S phase checkpoint kinases. Mol Cell **45:**696-704.
34. **Tran HT, Gordenin DA, Resnick MA.** 1999. The 3'-->5' exonucleases of DNA polymerases delta and epsilon and the 5'-->3' exonuclease Exo1 have major roles in postreplication mutation avoidance in Saccharomyces cerevisiae. Mol Cell Biol **19:**2000-2007.
35. **Zhou ZX, Zhang MJ, Peng X, Takayama Y, Xu XY, Huang LZ, Du LL.** 2013. Mapping genomic hotspots of DNA damage by a single-strand-DNA-compatible and strand-specific ChIP-seq method. Genome Res **23:**705-715.
36. **Kerkel K, Spadola A, Yuan E, Kosek J, Jiang L, Hod E, Li K, Murty VV, Schupf N, Vilain E, Morris M, Haghighi F, Tycko B.** 2008. Genomic surveys by methylation-sensitive SNP analysis identify sequence-dependent allele-specific DNA methylation. Nat Genet **40:**904-908.
37. **Waga S, Stillman B.** 1998. The DNA replication fork in eukaryotic cells. Annu Rev Biochem **67:**721-751.
38. **Bell SP, Dutta A.** 2002. DNA replication in eukaryotic cells. Annu Rev Biochem **71:**333-374.
39. **Marini F, Pellicioli A, Paciotti V, Lucchini G, Plevani P, Stern DF, Foiani M.** 1997. A role for DNA primase in coupling DNA replication to DNA damage response. EMBO J **16:**639-650.

555 40. **Tsurimoto T, Stillman B.** 1991. Replication factors required for SV40 DNA replication in vitro. II.
556 Switching of DNA polymerase alpha and delta during initiation of leading and lagging strand
557 synthesis. J Biol Chem **266:**1961-1968.
558 41. **Tsurimoto T, Stillman B.** 1991. Replication factors required for SV40 DNA replication in vitro. I.
559 DNA structure-specific recognition of a primer-template junction by eukaryotic DNA
560 polymerases and their accessory proteins. J Biol Chem **266:**1950-1960.
561 42. **Waga S, Stillman B.** 1994. Anatomy of a DNA replication fork revealed by reconstitution of SV40
562 DNA replication in vitro. Nature **369:**207-212.
563 43. **Georgescu RE, Langston L, Yao NY, Yurieva O, Zhang D, Finkelstein J, Agarwal T, O'Donnell ME.**
564 2014. Mechanism of asymmetric polymerase assembly at the eukaryotic replication fork. Nat
565 Struct Mol Biol **21:**664-670.
566 44. **Williams JS, Clausen AR, Lujan SA, Marjavaara L, Clark AB, Burgers PM, Chabes A, Kunkel TA.**
567 2015. Evidence that processing of ribonucleotides in DNA by topoisomerase 1 is leading-strand
568 specific. Nat Struct Mol Biol **22:**291-297.
569 45. **Stillman B.** 2015. Reconsidering DNA Polymerases at the Replication Fork in Eukaryotes. Mol Cell
570 **59:**139-141.
571 46. **Gros J, Kumar C, Lynch G, Yadav T, Whitehouse I, Remus D.** 2015. Post-licensing Specification of
572 Eukaryotic Replication Origins by Facilitated Mcm2-7 Sliding along DNA. Mol Cell **60:**797-807.

573
574

Legends

Figure 1. Schematic of the ChIP-ssSeq method used to detect the association of a protein with ssDNA. (A) The standard ChIP-seq process does not detect protein-ssDNA interactions. Here we use a protein that binds to both dsDNA and ssDNA as an example to elucidate the process. The upper shows a replication bubble. The first step is the protein ChIP. To prepare a library for sequencing, ChIPed DNA is extracted. After DNA end repair, only dsDNA is ligated with adaptors. Therefore, sequence reads contain location information for protein-dsDNA interactions. The target protein is shown as a gray ball. Black peak represent the DNA location. **(B)** The ChIP-ssSeq procedure preserves strand-specific information. The replication protein ChIP process is the same as the standard ChIP-seq. ChIP-ssSeq library preparation utilized a ssDNA ligase to ligate denatured ChIP ssDNA to a 3′ adaptor, which marks the same end of each ssDNA molecule. The second DNA strand is synthesized and extended with a 3′ complementary oligo. After end repair, the 5′ end is ligated to a 5′ end adaptor with T4 DNA ligase. After sequencing, the reads are mapped to the Watson and Crick strands of the yeast genome to determine the location of the target protein and strand-specific information. The red and green lines represent the Watson and Crick strands, respectively. ChIP-seq indicates chromatin immunoprecipitation and sequencing; ChIP-ssSeq, chromatin immunoprecipitation and strand-specific sequencing, dsDNA, double-stranded DNA; ssDNA, single-stranded DNA; * represents nucleotide analog BrdU, which is incorporated into nascent DNA during DNA replication. As a comparison, the outline for eSPAN procedures is shown in B. The eSPAN procedure involves immunoprecipitation of protein-associated newly synthesized DNA marked with BrdU using antibodies against BrdU. Therefore, eSPAN detects the association of a protein with nascent DNA at DNA replication forks.

Figure 2. RPA preferentially binds to ssDNA on the lagging strand template. (A) A snapshot of RPA ChIP-ssSeq peaks at 2 early replication origins, *ARS510* and *ARS511*. Log-phase cells were synchronized to G1 with α factor and then released into 0.2M HU for 45 minutes. G1 and early S-phase cells were collected for RPA ChIP-ssSeq. The RPA ChIP was performed using antibodies against the FLAG epitope, which was fused to the C-terminus of Rfa1 (the large subunit of the RPA complex). Similar results were obtained by using an Rfa1-specific antibody (data not shown). The red and green regions represent normalized sequence read density of the Watson and Crick strands, respectively. Rfa1 eSPAN peaks are included for comparison (12). **(B)** The average pattern of Rfa1 ChIP-ssSeq peaks shows positive bias. The average $\log_2$ ratios of sequence reads of Watson and Crick strands at 134 early replication origins were calculated using a 200-bp sliding window and then normalized against input values to obtain the average bias pattern (blue). The lagging strand bias pattern of Rfa1 eSPAN peaks (12) (red) was used for comparison. **(C)** The dot-and-box plot shows the bias pattern of Rfa1 ChIP-ssSeq peaks at individual origins. The ratio of sequence reads of lagging to leading strands was calculated at each of 134 early replication origins; each dot represents one origin. The colors represent 3 bias patterns: red for positive bias (+); green for negative bias (−); and blue for indeterminable. **(D)** Schematic of a mechanism that accounts for the positive bias pattern of RPA based on ChIP-ssSeq analysis and the lagging strand bias pattern based on eSPAN analysis. The yellow ball represents the RPA complex. * represents nucleotide analog BrdU, which is incorporated into nascent DNA during DNA replication. Please note that the eSPAN peak bias reflects whether a protein binds to nascent leading and lagging strand, whereas ChIP-ssSeq peak bias indicates that whether a protein binds to ssDNA or dsDNA.

Figure 3. Pol α preferentially binds the single-stranded lagging template of both active and HU-stalled replication forks. (A-C) Pol α ChIP-ssSeq peaks at HU-stalled forks exhibit a positive (+) bias pattern. **(A)** Snapshot of Pol α ChIP-ssSeq and eSPAN peaks at *ARS510* and *ARS511*. The signals represent normalized sequence read density. The red and green represents the Watson and Crick strands, respectively. **(B)** Analysis of the average bias pattern of Pol α ChIP-ssSeq. Pol α eSPAN was used for comparison. **(C)** Analysis of bias pattern of Pol α ChIP-ssSeq of HU-stalled and active replication forks at individual origins (early replication origins only). **(D-E)** Pol α ChIP-ssSeq peaks at active forks show positive strand bias. G1-synchronized yeast cells were released into fresh medium at 16°C in the presence of BrdU for 72 minutes. **(D)** Snapshot of Pol α ChIP-ssSeq and eSPAN peaks at *ARS510* and *ARS511*. **(E)** Analysis of the average bias of Pol α ChIP-ssSeq peaks at active forks. f, Schematic of a mechanism that shows why Pol α ChIP-ssSeq has a positive strand bias pattern. Red line: Watson strand, Green line: Crick strand.

Figure 4. Pol δ binds dsDNA at HU-stalled replication forks and preferentially binds lagging-strand template ssDNA of active forks. (A) A snap shot of Polδ ChIP-ssSeq at three origins (*ARS1511*, *ARS1512* and *ARS1513*) with HU or three time points without HU. G1-synchronized yeast cells were released into fresh medium at 16°C without HU. Samples at the indicated time points (72 min, 84min and 96min) samples were collected for Pol δ ChIP-ssSeq of active forks. Sample was collected at 45 minutes after G1 release into HU at 30 °C for Pol δ ChIP-ssSeq at HU-stalled forks. Please note that Polδ ChIP efficiency was relatively low

643 compared to Polε and Polα despite repeated attempts. **(B)** Pol δ ChIP-ssSeq peaks show positive
644 bias at active forks and no bias at HU-stalled forks. The average bias pattern of ChIP-ssSeq
645 peaks at 134 early replication origins is shown. The bias pattern indicated that Pol δ associates
646 with dsDNA, but associates with ssDNA more frequently at active forks **(C)** Dot-and-box plot
647 shows the bias pattern of Pol δ ChIP-ssSeq peaks at 134 individual early replication origins of
648 HU-stalled and active forks. Each dot represents one origin. **(D-E)** Schematics show the Pol δ-
649 DNA interaction at active forks **(D)** and HU-stalled forks **(E)**.

650

651 **Figure 5. Pol ε binds dsDNA at HU-stalled replication forks and preferentially binds**
652 **leading nascent ssDNA of active forks. (A-C)** Pol ε ChIP-ssSeq peaks show a positive bias
653 pattern at active forks and no bias at HU-stalled forks. The experiments were performed as
654 described in Fig. 4. except that Pol ε ChIP-ssSeq was performed. **(A)** a snap shot of Pol ε ChIP-
655 ssSeq peaks at *ARS1623*. **(B)** the average bias pattern of Pol ε ChIP-ssSeq peaks using a 200-bp
656 sliding window(early replication origins only). **(C)** Dot-and-box plot shows the bias pattern of
657 Pol ε ChIP-ssSeq peaks at 134 individual early origins. **(D-G)** The bias patterns of Pol ε ChIP-
658 ssSeq for HU-stalled and active fork are different. The bias patterns indicate that Pol ε associate
659 with dsDNA, but associates with ssDNA more frequently at active forks. **(D)** Flowchart of the
660 experimental procedure. Yeast cells arrested in G1 were released into HU for 45 minutes. A
661 fraction of cells were collected for Pol ε ChIP-ssSeq. The remaining cells were released into
662 fresh media after removal of HU. Samples were collected at the indicated time points after
663 release for Pol ε ChIP-ssSeq. **(E)** A snap shot of Pol ε ChIP-ssSeq peaks at *ARS1623* obtained
664 using HU arrested or released cells. **(F)** Analysis of the bias pattern of Pol ε ChIP-ssSeq peaks at

665 HU-stalled and active forks (3 time points after release). **(G)** Analysis of Pol ε ChIP-ssSeq peaks
666 at individual origins at active and HU-stalled forks. **(H-I)**. Schematics showing Polε at active **(H)**
667 and HU-stalled forks **(I)**. We propose that Polε binds to both template and nascent DNA of
668 active forks, but with a higher frequency to nascent DNA than template DNA, which leads to the
669 generation of Polε ChIP-ssSeq peak bias at active forks.

670
671

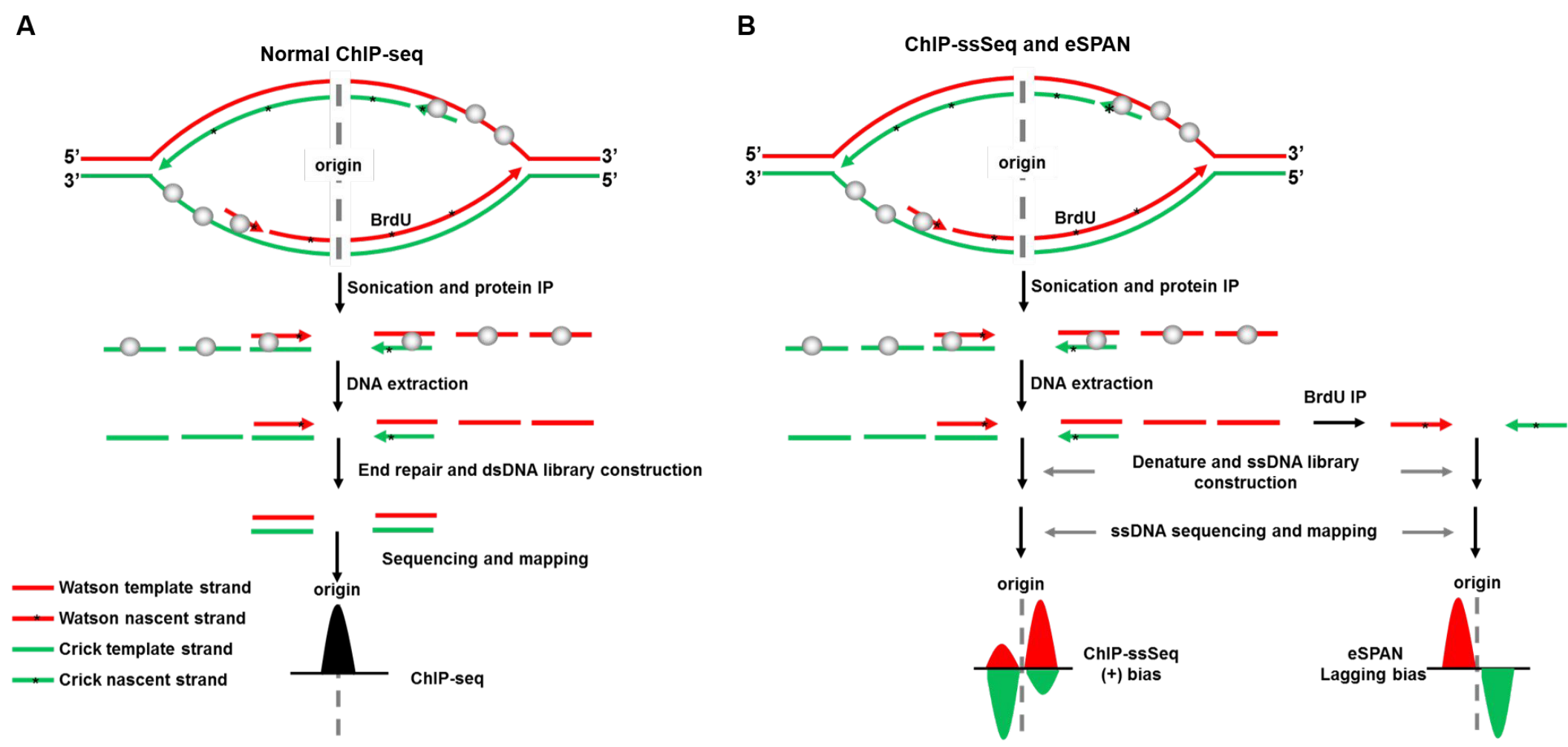
A
Normal ChIP-seq
5'
3'
origin
3'
5'
BrdU
Sonication and protein IP
DNA extraction
End repair and dsDNA library construction
Sequencing and mapping
origin
ChIP-seq
Watson template strand
Watson nascent strand
Crick template strand
Crick nascent strand
B
ChIP-ssSeq and eSPAN
5'
3'
origin
3'
5'
BrdU
Sonication and protein IP
DNA extraction
BrdU IP
Denature and ssDNA library construction
ssDNA sequencing and mapping
origin
ChIP-ssSeq
(+) bias
origin
eSPAN
Lagging bias

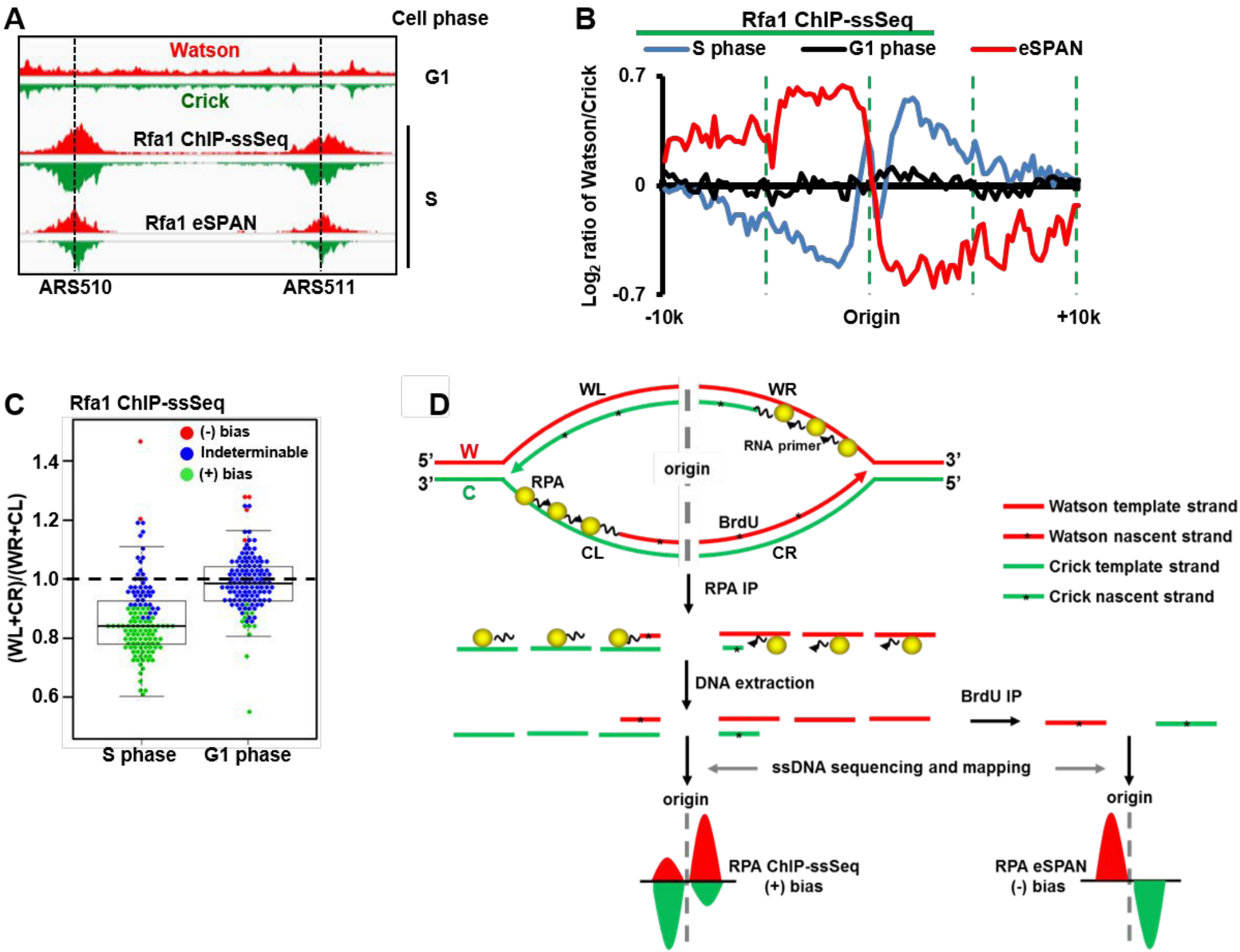
A
Cell phase
Watson
Crick
Rfa1 ChIP-ssSeq
Rfa1 eSPAN
G1
S
ARS510
ARS511
B
Rfa1 ChIP-ssSeq
S phase
G1 phase
eSPAN
Log2 ratio of Watson/Crick
0.7
0
-0.7
-10k
Origin
+10k
C
Rfa1 ChIP-ssSeq
(-) bias
Indeterminable
(+) bias
(WL+CR)/(WR+CL)
1.4
1.2
1.0
0.8
0.6
S phase
G1 phase
D
WL
WR
W
5'
3'
C
origin
RNA primer
3'
5'
RPA
BrdU
CL
CR
Watson template strand
Watson nascent strand
Crick template strand
Crick nascent strand
RPA IP
DNA extraction
BrdU IP
ssDNA sequencing and mapping
origin
origin
RPA ChIP-ssSeq
(+) bias
RPA eSPAN
(-) bias

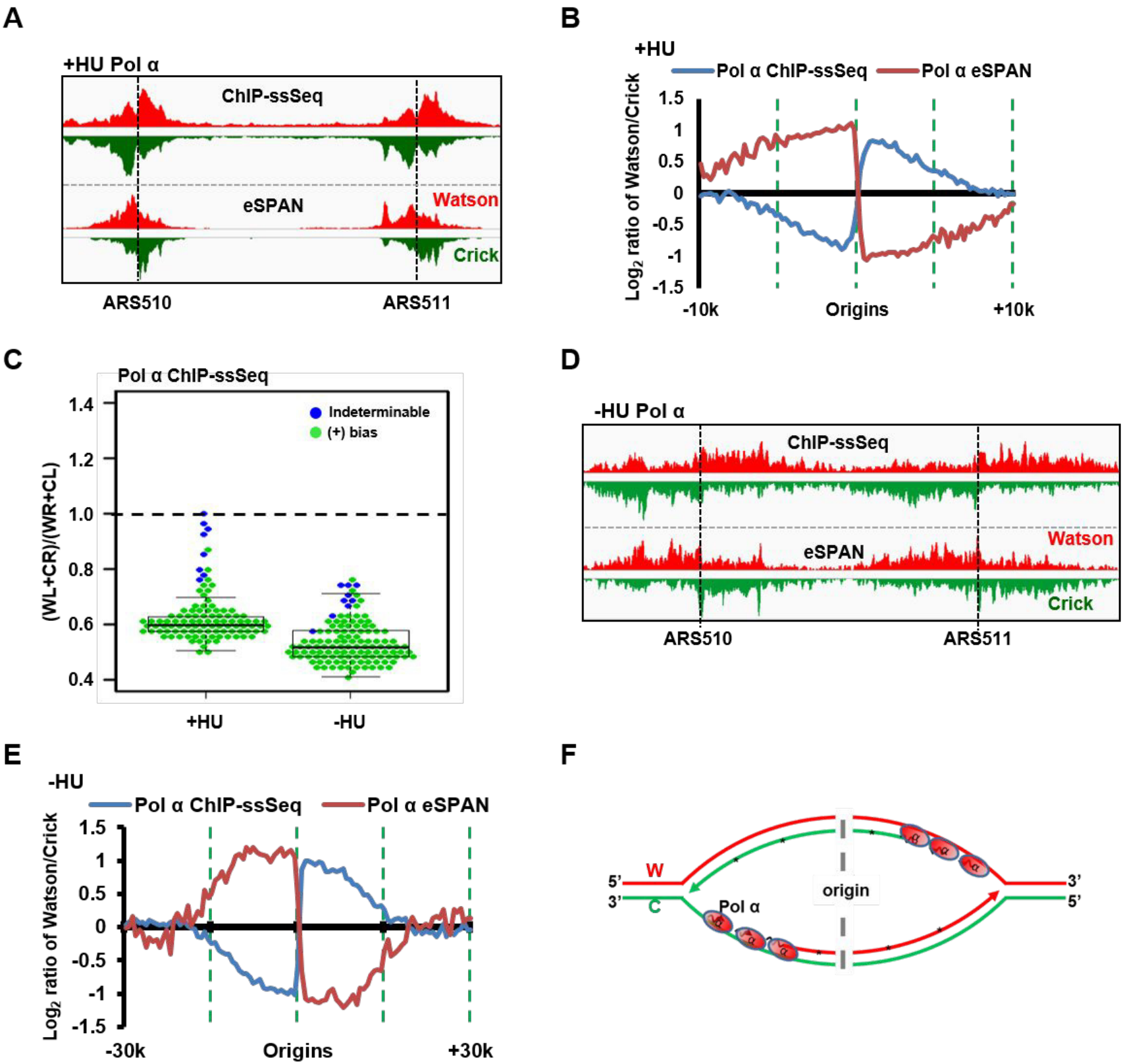
A
+HU Pol α
ChIP-ssSeq
eSPAN
Watson
Crick
ARS510
ARS511
B
+HU
Pol α ChIP-ssSeq
Pol α eSPAN
Log2 ratio of Watson/Crick
1.5
1
0.5
0
-0.5
-1
-1.5
-10k
Origins
+10k
C
Pol α ChIP-ssSeq
Indeterminable
(+) bias
(WL+CR)/(WR+CL)
1.4
1.2
1.0
0.8
0.6
0.4
+HU
-HU
D
-HU Pol α
ChIP-ssSeq
eSPAN
Watson
Crick
ARS510
ARS511
E
-HU
Pol α ChIP-ssSeq
Pol α eSPAN
Log2 ratio of Watson/Crick
1.5
1
0.5
0
-0.5
-1
-1.5
-30k
Origins
+30k
F
W
C
5'
3'
3'
5'
origin
Pol α

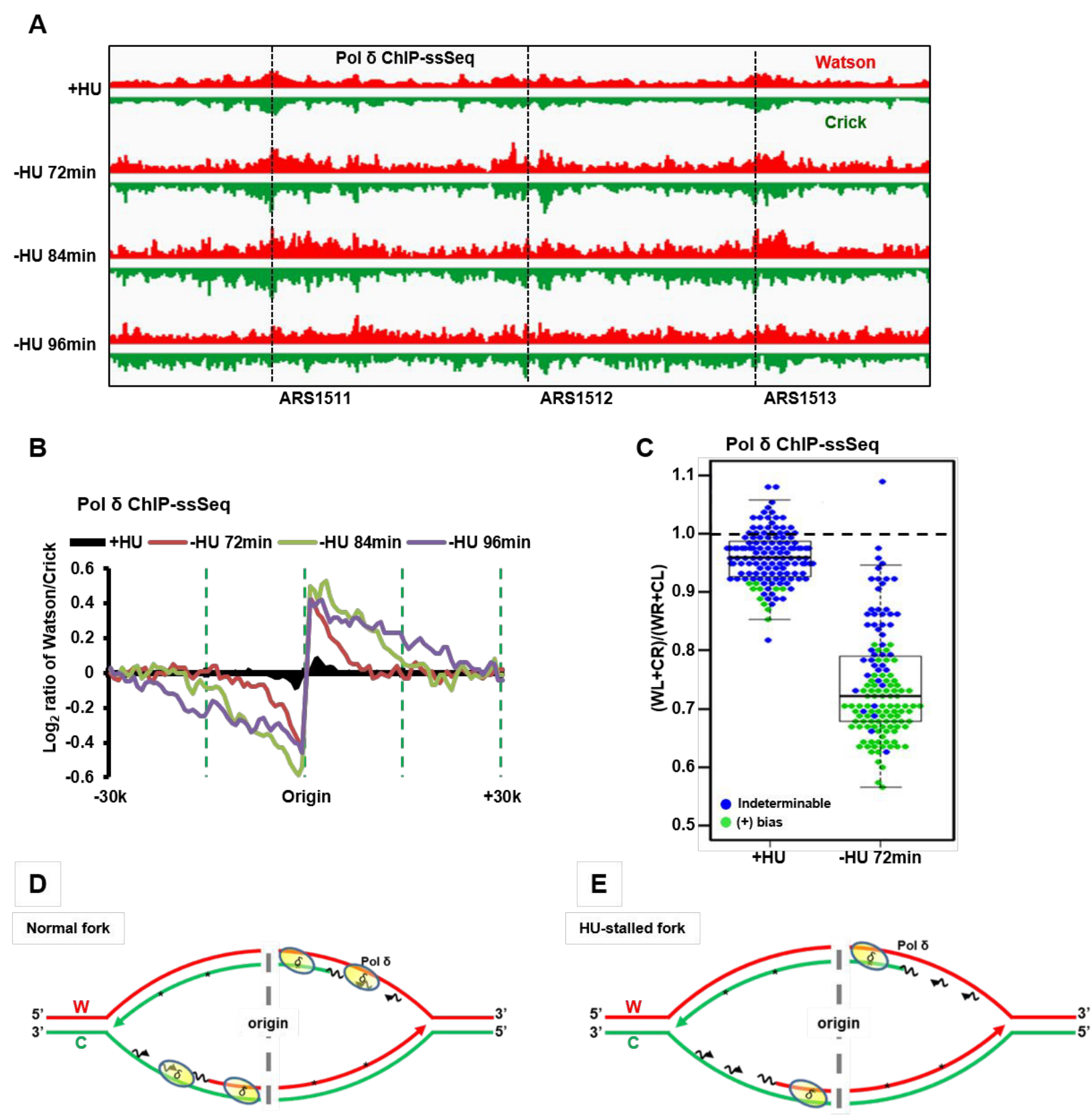
A
Pol δ ChIP-ssSeq
Watson
Crick
+HU
-HU 72min
-HU 84min
-HU 96min
ARS1511
ARS1512
ARS1513
B
Pol δ ChIP-ssSeq
+HU
-HU 72min
-HU 84min
-HU 96min
Log2 ratio of Watson/Crick
0.6
0.4
0.2
0
-0.2
-0.4
-0.6
-30k
Origin
+30k
C
Pol δ ChIP-ssSeq
(WL+CR)/(WR+CL)
1.1
1.0
0.9
0.8
0.7
0.6
0.5
Indeterminable
(+) bias
+HU
-HU 72min
D
Normal fork
Pol δ
W
C
5'
3'
origin
3'
5'
E
HU-stalled fork
Pol δ
W
C
5'
3'
origin
3'
5'

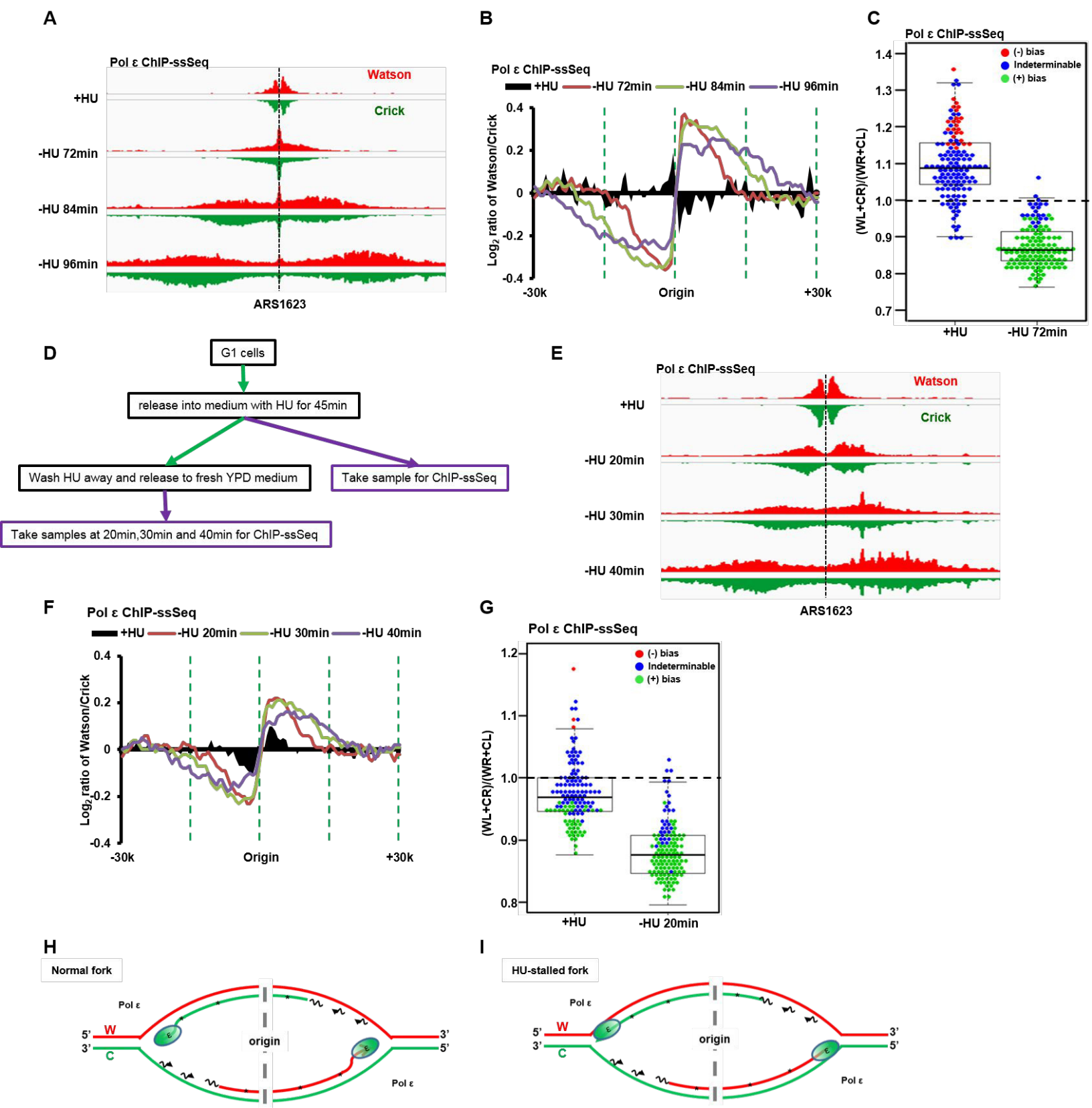
A
Pol ε ChIP-ssSeq
Watson
Crick
+HU
-HU 72min
-HU 84min
-HU 96min
ARS1623
B
Pol ε ChIP-ssSeq
+HU
-HU 72min
-HU 84min
-HU 96min
Log2 ratio of Watson/Crick
-30k
Origin
+30k
C
Pol ε ChIP-ssSeq
(-) bias
Indeterminable
(+) bias
(WL+CR)/(WR+CL)
+HU
-HU 72min
D
G1 cells
release into medium with HU for 45min
Wash HU away and release to fresh YPD medium
Take sample for ChIP-ssSeq
Take samples at 20min,30min and 40min for ChIP-ssSeq
E
Pol ε ChIP-ssSeq
Watson
Crick
+HU
-HU 20min
-HU 30min
-HU 40min
ARS1623
F
Pol ε ChIP-ssSeq
+HU
-HU 20min
-HU 30min
-HU 40min
Log2 ratio of Watson/Crick
-30k
Origin
+30k
G
Pol ε ChIP-ssSeq
(-) bias
Indeterminable
(+) bias
(WL+CR)/(WR+CL)
+HU
-HU 20min
H
Normal fork
Pol ε
W
C
origin
Pol ε
I
HU-stalled fork
Pol ε
W
C
origin
Pol ε